Arch. Metall. Mater. **63** (2018), 3, 1225-1233

DOI: 10.24425/123795

C. KÖSE*#, E. KARACA**

EFFECT OF PRE AND POST WELD HEAT TREATMENTS ON THE MICROSTRUCTURE AND MECHANICAL PROPERTIES OF FIBER OPTIC BEAM DELIVERY SYSTEM ASSISTED ROBOTIC Nd: YAG LASER WELDED Ti-6Al-4V ALLOY

In the present study, Ti6Al4V titanium alloy plates were joined using robotic laser welding method. Pre- and post-weld heat treatments were applied to laser welded joints. After welding stress relieving, solution heat treatment and ageing were also applied to preheated laser welded samples. Effects of heat treatment conditions on microstructural characteristics and mechanical properties of robotic laser welded joints were studied. Aged samples were found to be made of coarsened grains compared to microstructures of non-aged samples. There were increases in ductility and impact toughness of samples applied to ageing increased, while hardness and tensile strength of non-aged samples were higher. The highest value for tensile strength and for impact toughness in welded samples have been identified as 840 MPa and 27 J, respectively. Fractures in tensile test samples and base metal impact test samples took place in the form of ductile fracture, while laser welded impact test samples had fractures in the mode of intergranular fractures with either a quasi-cleavage type or tear ridges. EDS analysis carried out for all heat treatment conditions and welding parameters demonstrated that major element losses were not observed in base metal, HAZ and weld metal.

Keywords: Titanium alloy; robotic laser welding; heat treatment; microstructure; mechanical properties

1. Introduction

Titanium alloys can be classified in three major groups; α (alpha), $\alpha+\beta$ and β (beta) alloys. The entire structure of α alloys is made of α phase, while the structure of β alloys is predominantly made of β phase, which can be achieved through cooling starting from solution temperature. $\alpha+\beta$ alloys, on the other hand, have both α and β phases at room temperature [1]. Ti6Al4V is the most commonly used $\alpha+\beta$ alloy. Ti6Al4V has a wide range of uses due to its low density, high thermal, mechanical strength, corrosion resistance and biocompatibility [2-5]. These strength and light alloys are used in many applications such as jet engines, spacecraft, missiles, pressure vessels, orthodontics, medical implants and surgical tools [6,7].

Ti6Al4V alloy can be joined by many methods such as TIG, friction welding, friction stir welding, plasma arc, electron beam and laser beam welding [2,7,8]. Laser welding method is different from traditional welding methods by its lower heat input, higher condensation energy, faster welding speed, narrower welding area, its ability to produce joints with deeper penetration, its higher mechanical strength, lower distortion and its ability to weld without use of additional filler welding metal [9-16]. On the other hand, fiber optic beam delivery system assisted laser welding method offers lower beam distortion rate, flexible beam distribution, lower maintenance cost, higher efficiency and high quality welded joints [17].

Slower cooling due to high heat input in welding of titanium and its alloys leads to grain coarsening in welding seam. In welding of titanium and its alloys, heat input conducted to weld zone should be lowered, cooling should be increased and a narrow welding seam shape should be obtained. Ti6Al4V titanium alloys show fine grained prior-β grain formation in their welding seam when they are joined with electron beam and laser. Also, low heat input and fast cooling lead to improved mechanical strength [8]. However, in the case of fast cooling of welding seam, predominant martensitic structure develops [18,19]. Martensitic structure leads to decreases in toughness of welding seam compared to that of base metal [18,20]. Ductility losses in weld metal and heat-affected zone (HAZ) could be improved by rearrangement through heat treatment after welding [20]. It is suggested that post-weld heat treatment of $\alpha+\beta$ titanium alloys with low ductility should be carried out at temperatures lower than β transus temperature [21]. Stress relieving applied to welded joints of titanium and its alloys does not have any adverse effect on strength and ductility. With stress relieving preheating, internal stresses that could develop during cooling of welding seam are decreased. On the other hand, post-weld heat treatments applied to welded joints of titanium and its alloys such as solution heat treatment and ageing improve fracture toughness, ductility, corrosion resistance and resistance to high heat of welded joints [1].

* GAZIOSMANPAŞA UNIVERSITY, DEPARTMENT OF MECHANICAL ENGINEERING, FACULTY OF NATURAL SCIENCES AND ENGINEERING, TOKAT, 60150, TURKEY
** GAZIOSMANPAŞA UNIVERSITY, DEPARTMENT OF MECHATRONICS ENGINEERING, GRADUATE SCHOOL OF NATURAL AND APPLIED SCIENCES, TOKAT, 60150, TURKEY
# Corresponding author: ceyhun.kose@gop.edu.tr, ceyhunia@gmail.com

When similiar studies are investigated from literature, following studies can be utilized. Kabir et al joining Ti-6Al-4V alloy using filler welding metal and investigating heat treatment properties of laser welded joints identified that besides of heat treatment, underfill and porosity formations had an effect of mechanical properties [8]. Mohandas et al joining $\alpha+\beta$ titanium alloy using electron beam welding and investigating heat treatment properties of welded joints identified that increase of strength against fractures of welded joints were linked with improving of ductility and acicular microstructure transformation with the effect of heat treatments after welding [22]. In a similar study of Mohandas et al, they identified that low porosity formation occurred in weld metal with slow welding travel speed and highest porosity formation occurred with intermediate welding travel speed [23]. Karimzadeh et al investigating effects of heat treatment on corrosion properties of TIG welded Ti-6Al-4V alloy found that heat treatment improves corrosion resistance of welded joints but does not have a significant effect on base metal [2]. Thomas et al joining Ti-6Al-4V alloy using TIG welding and investigating heat treatment properties of welded joints identified that performing post weld heat treatments in low temperatures do not have an important effect on ductility of welded joints and this seems to be the most important result [20]. Liu et al joining Ti-6Al-4V alloy using laser welding and investigating heat treatment properties of welded joints identified that stress corrosion resistance increases in case of rise in post weld heat treatment temperature and heat treatment improves mechanical strength [19]. Anil Kumar et al joining $\alpha+\beta$ titanium alloy using electron beam welding and investigating heat treatment properties of welded joints identified that optimum properties are reached in solution treated + aged heat treatment conditions [24].

Welded joints of Ti6Al4V alloys have been in literature but there have not been enough studies investigating effects of pre and post weld heat treatment on microstructure and mechanical properties of fiber optic beam delivery system assisted robotic Nd:YAG laser beam welding. In the present study, Ti6A14V plates were joined using robotic Nd:YAG fiber laser welding. Preheating was performed before welding and two different heat treatment procedures were used after welding. Effects of heat treatments on microstructure and mechanical properties of fiber laser welded Ti6A14V alloy were investigated.

2. Experimental studies

2.1. Material, welding and heat treatment procedures

In the present study, Ti6A14V alloy preferred in many industrial areas was used. Chemical composition of Ti6Al4V alloy used in the study was identified with spectral analysis method.

Chemical composition of the alloy was given in Table 1.

Experimental material was prepared in 100×330×4 mm^3 sizes and made ready for welding procedure. Experimental materials were joined using a FANUC ROBOT R-2000 iB 210F Nd:YAG laser welding machine of 4 kW power. Welding was performed in flat position without any additional welding metal using the parameters given in Table 2. Heat treatments were performed before and after the welding using parameters given in Table 3.

TABLE 1

The chemical composition of Ti6Al4V (weight%)

C%	Al	V	Fe	N	O	H	Ti
0.010	6.02	4.14	0.098	0.007	0.12	0.0020	Balanced

TABLE 2

The laser welding parameters

Sample	Laser power (W)	Travel speed (mm/s)	Shielding gas	Gas pressure (bar)	Focal length (mm)	Heat input (kJ/mm)
A1	1500	6	He	1	190	0.25
A2	1500	9	He	1	190	0.16
B1	2000	6	He	1	190	0.33
B2	2000	9	He	1	190	0.22

TABLE 3

The heat treatments

Sample	Heat treatment conditions
A1	Preheating for 350°C/20 min + Stress relieving for 720°C/1 h /air cooling + Solution treatment for 920°C/1 h/air cooling + ageing for 650°C/2 h /air cooling
A2 Base metal (A)	
B1	Preheating for 350°C/20 min + Stress relieving for 720°C/1 h /air cooling + Solution treatment for 920°C/1 h/air cooling
B2 Base metal (B)	

2.2. Mechanical tests and characterization of microstructure

For determination of mechanical properties of welded joints, four samples were prepared for each parameter based on ISO 4136:2012 tensile tests (Fig. 1) and ISO 9016: 2012 impact notch test. Tensile test was carried out using an INSTRON tensile test machine of 100 kN capacity at a rate of 10 mm/min crosshead speed. Impact notch test was performed at room temperature using an ALŞA testing machine. Hardness measurement, on the other hand, was performed by a GALILEO test machine applying 200 g weight for 15 seconds to tip.

For determination of microstructural changes in heat treated samples, etching procedure was used using Kroll's solution. Microstructural examinations were performed using a NIKON optical microscope with 5×-100× magnification, JEOL JSM 6060 LV and JEOL JSM 7001 LV scanning electron microscope (SEM), and OXFORD X-MAX 80 (EDS) equipment.

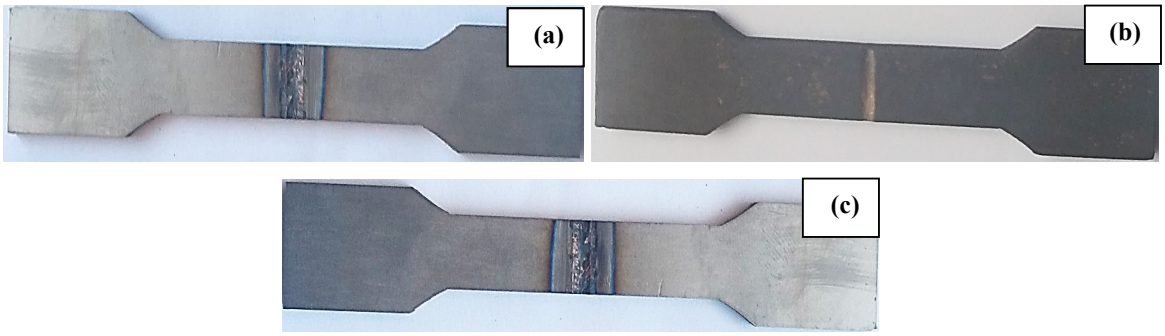

Fig. 1. Tensile test samples of robotic laser welded joint, (a) and (b) underfill formation in non-heat treated and heat treated samples, (c) full penetration in welded sample

3. Results and discussion

3.1. Microstructural examinations

It was observed that microstructure of base metals (sample A and sample B) was made of coaxial α grains and β grains in grain boundaries (Fig. 2a and 2c optical microscopy images, Figure 2b and 2d SEM images).

Post-weld heat treatment procedure is intended to provide the material with thermodynamic equilibrium. After heat treatments, microstructures of $\alpha+\beta$ titanium alloys joined using laser beam welding or electron beam welding show β phase in martensite phase or precipitations of α phase are found as remains in microstructure. As the duration or temperature of heat treatment increases, grain coarsening takes place as a result of over-ageing [18]. It is clearly seen in Figure 3 optical microscopy images that grain structure of welded joint which was subjected to ageing treatment coarsened grains more than microstructure of base metal and non-aged weld.

The microstructural change occurring after heat treatment is expected to slightly lower the tensile strength of laser welded joints and to increase the ductility in weld zone. Since the heat inputs of samples joined with different welding speed and of aged samples (samples A1 and A2) were similar, microstructures of weld metal and HAZ were similar too. (Fig. 2a-d). A similar situation was evident in non-aged samples (samples B1 and

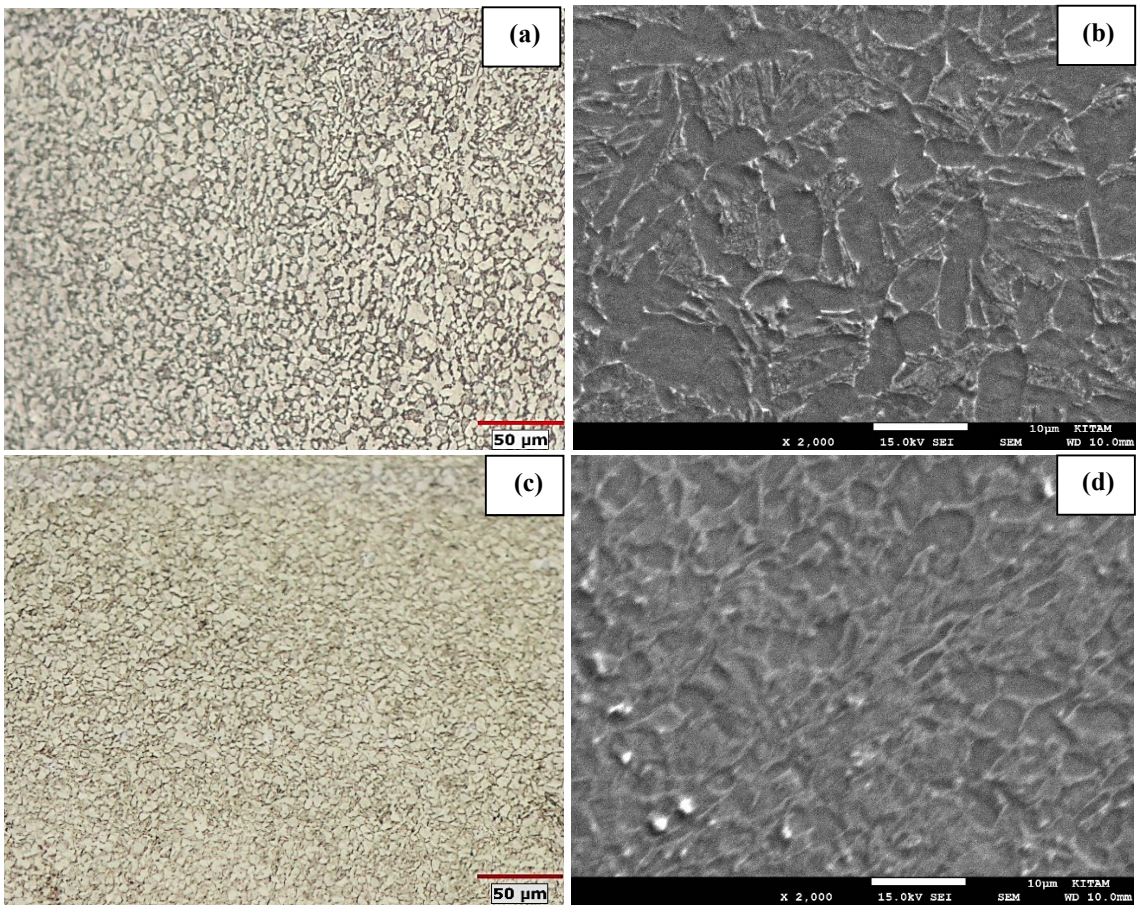

Fig. 2. Microstructure images of base metal, (a) and (b) Sample A, (c) and (d) Sample B

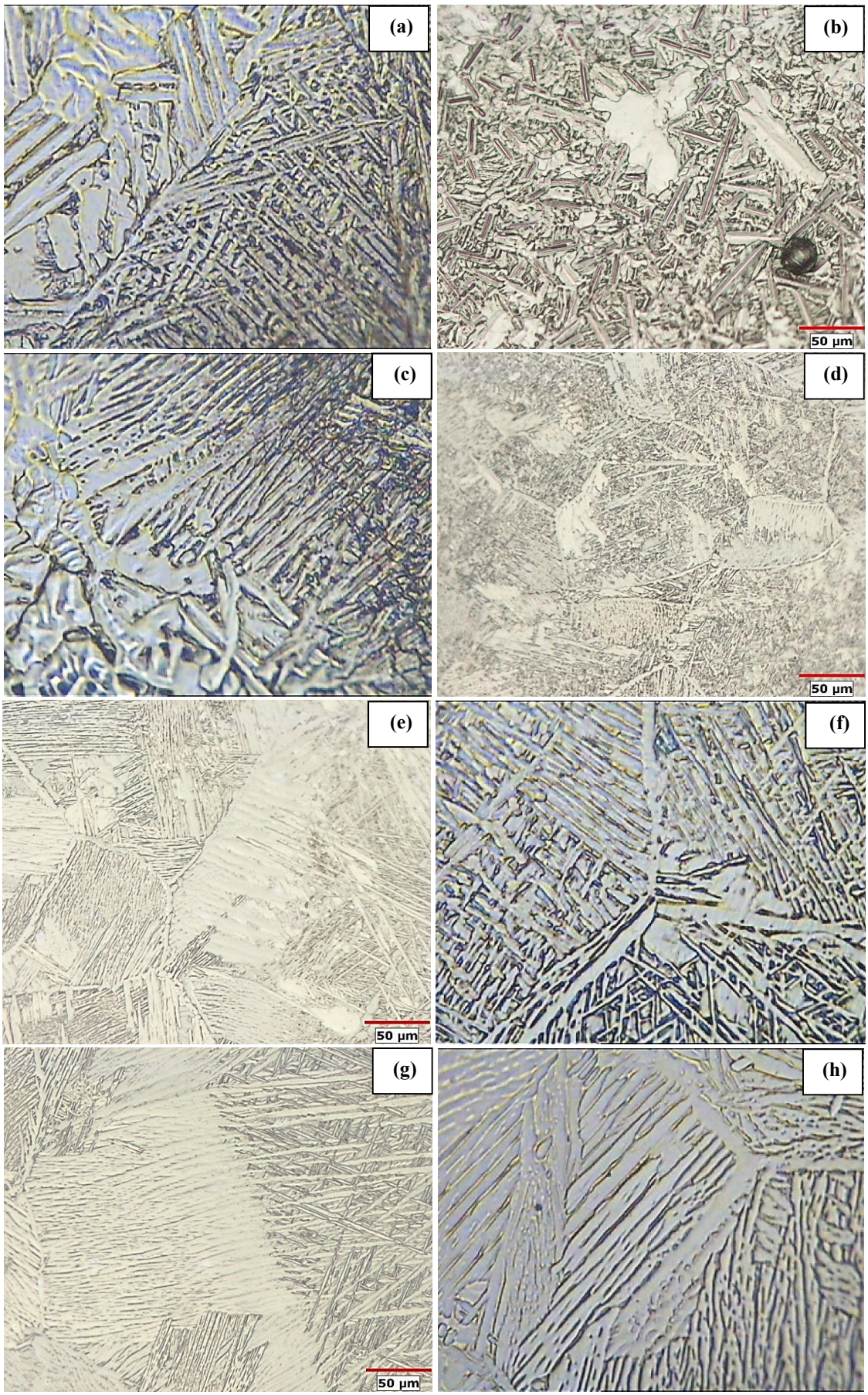

Fig. 3. Microstructure images of welded joint, (a) HAZ at 1000× magnification and (b) weld metal of sample A1 at 200× magnification, (c) HAZ at 1000× magnification and (d) weld metal of A2 at 200× magnification, (e) HAZ at 200× magnification and (f) weld metal of sample B1 at 1000× magnification, (g) HAZ at 200× magnification and (h) weld metal of sample B2 at 1000× magnification

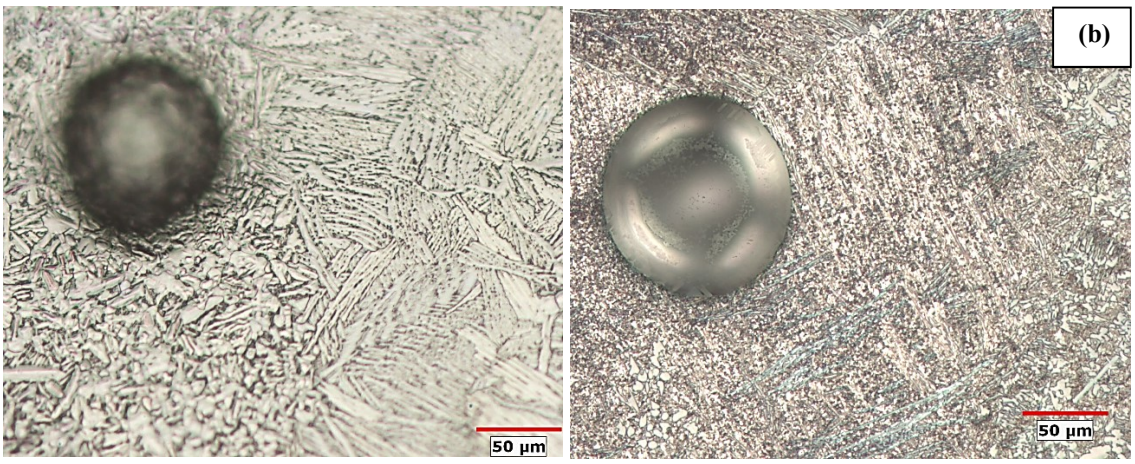

Fig. 4. Porosity formation in the weld metal of A1 and B1 samples

B2) in Figure 2e-h. A narrow HAZ formation was observed in all of laser welded joints. Clear grain coarsening, lamellar $\alpha+\beta$ phase structure and basket-weave Widmanstatten grain structure formation in grain boundaries of $\alpha+\beta$ phase in weld metal and HAZ were observed in microstructure of laser welded samples, especially in weld metal, with or without ageing heat treatment as a result of high temperature and prolonged treatment. As expected, grain coarsening took place more efficiently in aged samples A1 and A2 (Fig. 3). Since temperature of heat treatment was lower than β transus temperature, a complete transformation of α boundary structure to β phase was not expected. The grain boundary α phase may not fully been transformed into β, but it will be incorporated with the α platelets in the transformed β during the cooling and aging that follow [8,25]. It was observed that transformed β volume ratio increased in aged samples. Porosity formations were observed in welding seam (Fig. 3b and Fig. 4a and 4b). Porosity formation is a common occurrence in laser welded titanium alloys. Gas porosities generally form due to the fact that hydrogen in welding pool cannot be removed efficiently especially during solidification of welding seam [26]. Porosity formation is expected to lower mechanical strenght of welded joints.

EDS analysis performed for all heat treatment conditions and welding parameters (Fig. 5) revealed that major element losses were not observed in base metal, HAZ and weld metal. These findings indicated that heat input or heat treatments did not exert a negative effect on laser welded joints concerning alloying elements evaporation. Greater element losses were identified in aged samples compared to the ones in non-aged samples.

3.2. Tensile test

Tensile test was performed to determine mechanical properties of heat treated base metal and laser welded samples and results were given in Table 4.

Results of tensile test showed that as a result of microstructural transformations with the effect of heat treatment, tensile strength of non-aged base metal (sample B) was higher than aged base metal (sample A), (1039 MPa and 1025 MPa, respectively). Elongation of non-aged base metal B was lower than aged base metal A (18% and 20%, respectively). Tensile strengths of B1 and B2 laser welded samples were higher than those of A1 and A2 laser welded samples (840 MPa, 796 MPa, 770 MPa and 791 MPa, respectively). Main reason for lower tensile strength but higher ductility of aged samples (samples A1 and A2) was formation of coarse α grains and presence of tempered martensite due to heat treatments. Lower tensile strength as a result of formation of coarse grains and tempered martensitic phase was also reported in another study [21]. Tensile strengths of welded joints in all heat treatment conditions were lower than those of base metal. Fractures in welded joints occurred in weld zone after the tensile test. Among the reasons for such a finding are possible porosities in welding seam, underfills, microcracks and microstructural transformations. Underfill is the main and most damaging defect in laser welded Ti-6Al-4V alloy [8]. Laser welded joints are expected to have higher ductility as a result of finer β grains in their microstructure [27,28]. Despite the coarsening of α platelets in welding seam microstructure, lamellar structure resulted in lower tensile strength and ductility in the present study. The authors mentioned that lower ductility of welded joints compared to base metal can arise from stable lamellar structure in microstructure of weld metal after post-weld heat treatment [21,29]. In addition, some authors reported that yield and tensile strengths decreased and ductility increased

TABLE 4

The tensile test results of base metal and laser welded samples in heat treated conditions

Sample	Tensile strength (MPa)	Yield strength (MPa)	Elongation (%)	Fracture Location
A	1025	944	20	
B	1039	955	18	
A1	770	736	13	HAZ
A2	791	730	12	HAZ
B1	796	751	11	HAZ
B2	840	785	10.5	Weld metal

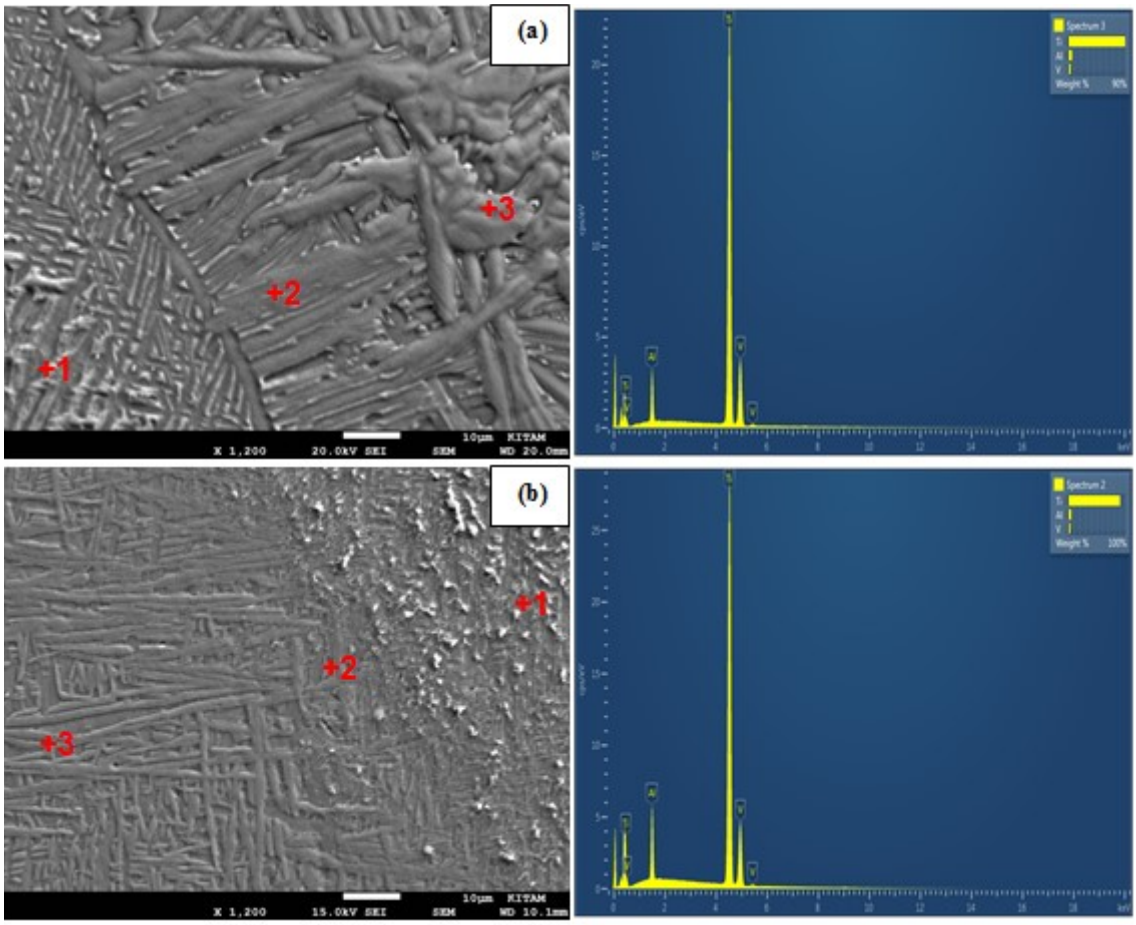

EDS analysis (wt.%)	Al	V	Ti
Point number + 1 base metal	5.47 – 5.30	4.91 – 4.82	89.62 – 89.59
Point number + 2 HAZ	5.61 – 5.34	4.00 – 3.98	90.39 – 90.22
Point number + 3 weld metal	5.42 – 5.39	4.31 – 4.22	90.27 – 90.34

Fig. 5. EDS analysis of base metal, HAZ and weld metal, respectively (a) Sample A1, (b) Sample B1 (weight%)

due to transformation of stronger martensite and Widmanstatten α structure into lamellar $\alpha - \beta$ grain structure as a result of ageing applied after welding [8,18,20]. Among laser welded samples, the highest yield strength was observed in B2 and the lowest in A2 samples (785 MPa, 751 MPa, 736 MPa and 730 MPa, respectively) while the lowest ductility was observed in B2 and the highest in A1 samples (13%, 12%, 11% and 10.5%, respectively). It has been reported that there could be decreases in impact/fracture strength and yield strength of welded joints due to formation of irregular shaped β grains compared to base metal [30]. Microsegregations that could develop during the solidification of welding seam are also among the factors that decrease ductility. Although tensile strength was slightly higher in samples joined using increased welding speed or lower laser power, it was concluded in general that there were no major differences in tensile strength between samples joined using different welding parameters and between samples subjected to two different heat treatments. The main reasons for these were presence of porosities and the fact that heat treatment took place under β transus temperature and thus no major changes occurred in the sizes of prior- β grains. In addition, it could be stated that homogeneity was achieved in tensile strength of welded joints via heat treatments and this homogeneous distribution could be expected to have an effect on microhardness results.

SEM images of fracture surfaces of base metals (samples A and B) and laser welded samples after tensile test (Fig. 6) clearly revealed that fractures occurred in the form of ductile fracture which is typical to heat treated titanium alloy as evident by dimples. No inclusion formation was observed in fracture surface images of laser welded joints.

3.3. Charpy V-notch impact test

Impact toughness of base metal and laser welded samples in room temperature were determined and given in Figure 7.

Impact toughness of aged base metal A was higher than that of non-aged base metal B (21J and 19J, respectively). Impact toughness of base metals (samples A and B) were lower than those of laser welded joints. Volume of intra-granular α grains in the microstructure of welding seam increased as a result of heat treatment after welding, thereby increasing the impact toughness

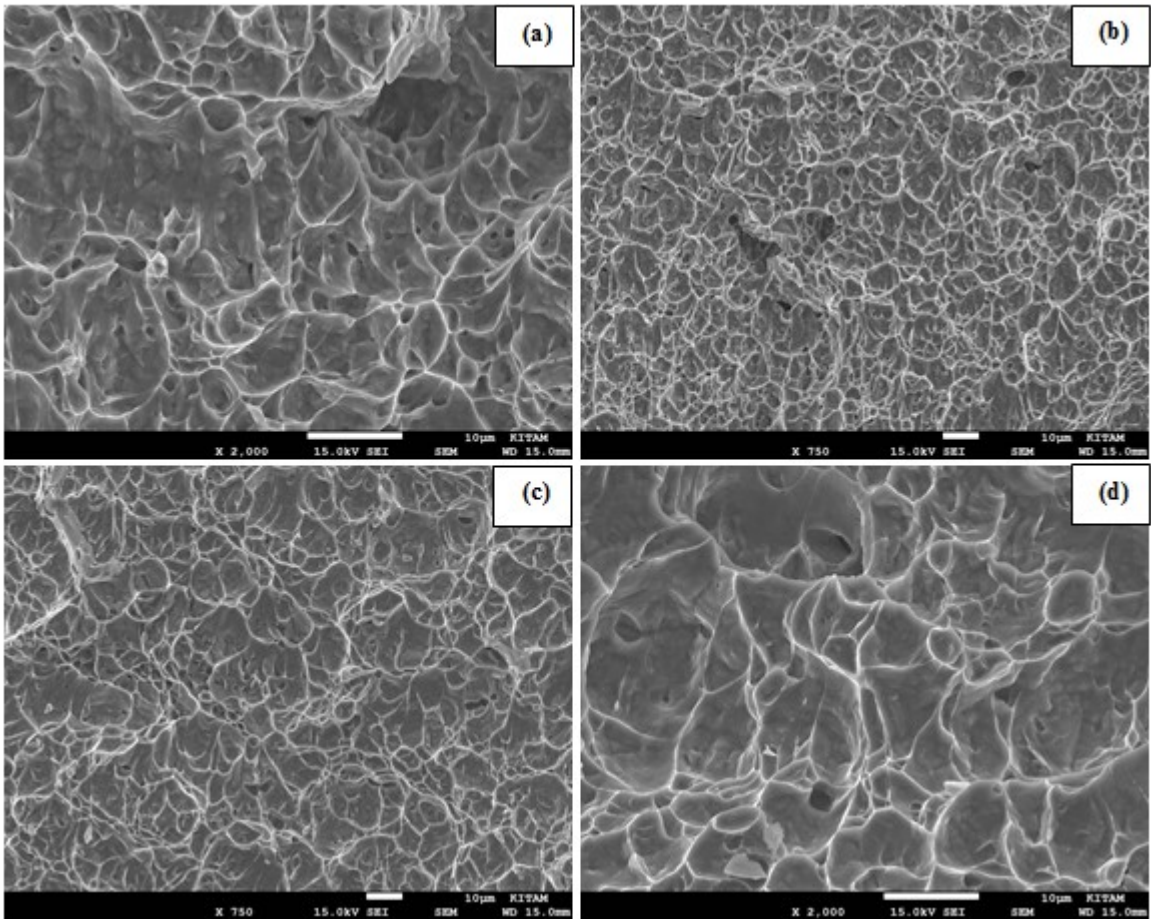

Fig. 6. Fracture surface images of base metal and laser welded samples after the tensile test, (a) Sample A, (b) Sample B, (c) Sample A1, (d) Sample B1

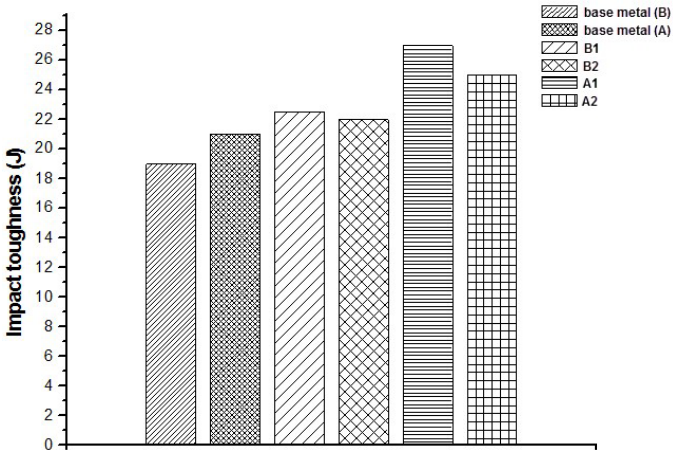

Fig. 7. The Charpy V-notch impact test results of base metal and laser welded samples

[31]. In addition, impact toughness also appeared to improve along with the increase in ductility through transformation of martensite to $\alpha+\beta$ phase structure. Some studies reported that impact toughness could be improved through heat treatment after welding via coarsening of α grain boundaries and changing the direction of crack movement in grain boundaries [20,31,32]. Higher impact toughness was observed in welded samples with lower welding speed or higher laser power, i.e. higher heat input (samples B1 and A1), and aged samples (samples A1 and A2) (22J, 22.5J, 25J and 27J, respectively). Investigators who obtained similar results stressed that in order to increase impact toughness of titanium alloys, martensitic structure should be transformed into acicular α or Widmanstatten α grain structure via increasing heat input using lower welding speed or higher laser power [33].

Fracture surfaces of base metal and welded samples after impact test were studied using SEM (Fig. 8). The base metal sample A and sample B were broken in ductile fracture mode, while A1 and B1 samples had fractures in the mode of intergranular fractures with either a quasi-cleavage type or tear ridges.

3.4. Microhardness

Laser welding ensures higher hardness levels in welded joints due to its higher power intensity, lower heat input and realization of rapid solidification compared to traditional welding methods. In terms of average hardness of heat treated samples joined using different welding speed and laser power i.e., using different heat input (Fig. 9), hardness of weld metal and HAZ was higher than that of base metal.

It was found out that the maximum hardness was in weld metal. The main reason for weld metal to be harder than HAZ

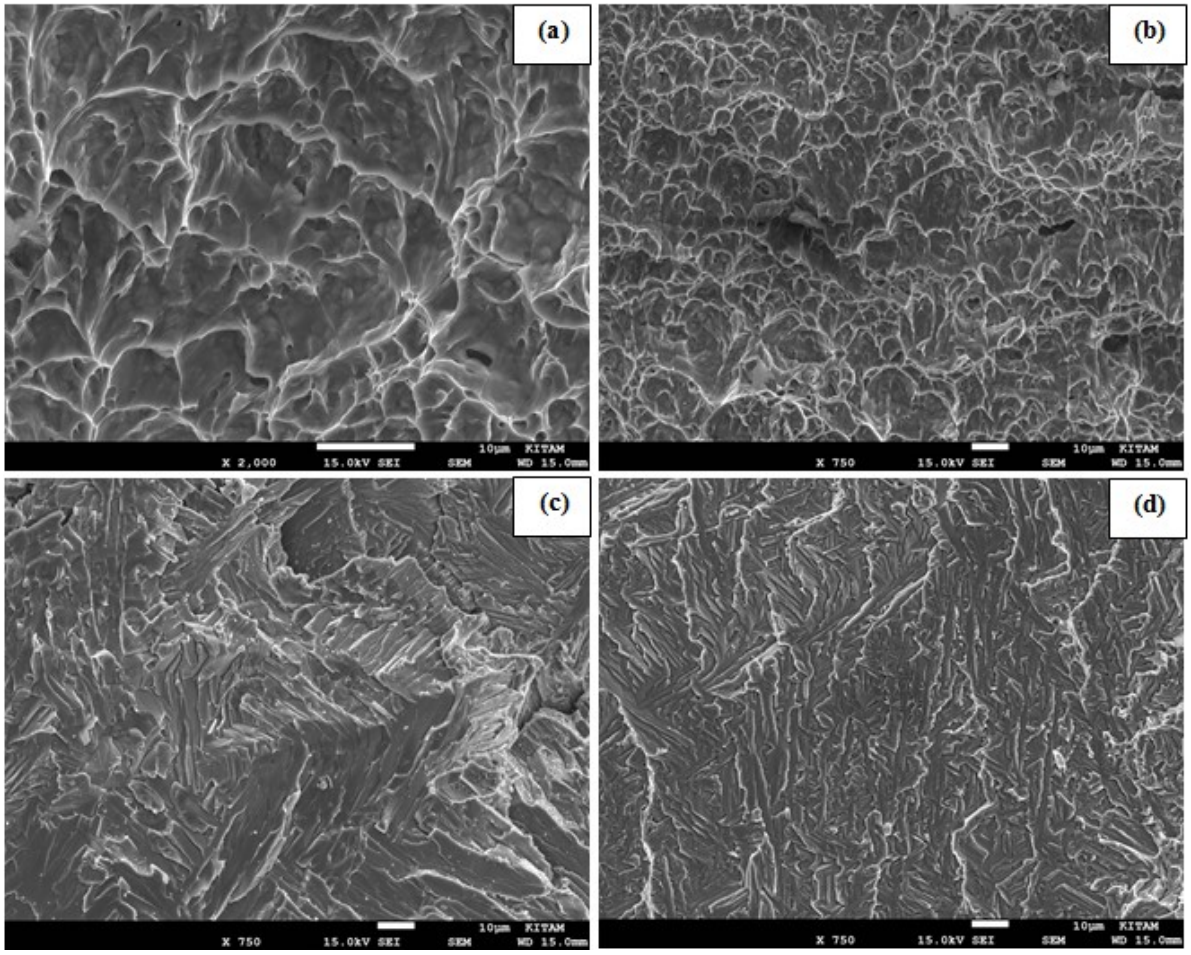

Fig. 8. Fracture surface images of base metal and laser welded samples after The Charpy V-notch impact test, (a) Sample A, (b) Sample B, (c) Sample A1, (d) Sample B1

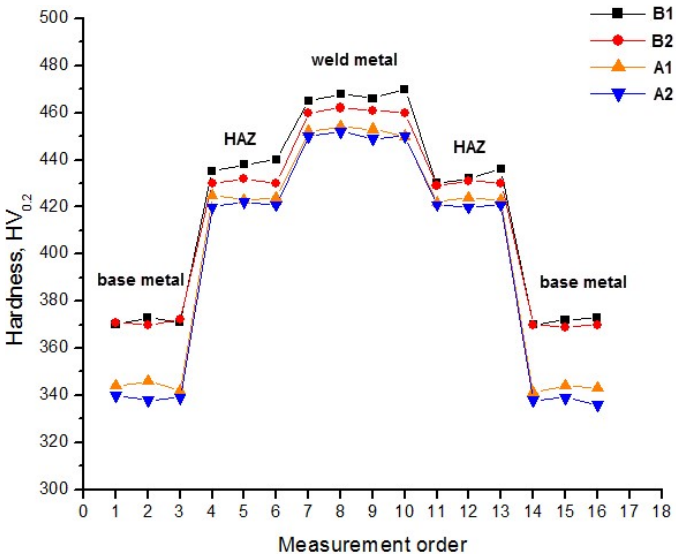

Fig. 9. Microhardness distributions in the welded joints

was that this region was made of finer structured grains. Hardness increases are expected in HAZ and weld metal compared to base metal after post-weld heat treatments because of transformation of martensite to $\alpha+\beta$ phase structure and transformation of phase platelet from retained β phase [8]. β phase is softer and more ductile than α phase. It has been reported that through post-weld heat treatments, a hardness increase could be experienced especially in weld metal as a result of decreasing β phase structure [8]. Hardness of laser welded samples subjected to ageing heat treatment (samples A1 and A2) were somewhat lower than that of non-aged samples (samples B1 and B2). A loss in hardness could arise through transformation of martensite phase to α, β phase structure and coarsening of grain structure, and it has been specifically mentioned that increasing temperatures in post-weld heat treatments would lower hardness [25]. Higher hardness of HAZ and weld metal compared to base metal is expected to produce welded joints more strength than base metal. Hardness results are expected to be associated with tensile strength results. Nevertheless, such was not the case with the present study due to the presence of porosities or microcrack formations in weld metal and HAZ.

Conclusions

1. A clear grain coarsening in weld metal and HAZ, basket-weave Widmanstatten grain structure formations in lamellar $\alpha+\beta$ phase structure and grain boundaries of α phase took place especially in weld metal microstructure of laser weld-

ed samples with or without ageing heat treatment as a result of higher temperature and longer duration of treatment. As expected, grain coarsening occurred more efficiently in aged samples. According to EDS analysis results greater element losses were identified in aged samples compared to the ones in non-aged samples.

2. In all heat treatment conditions, tensile strengths of welded joints were lower than the base metal. Among the reasons for such a finding could be the porosities that occurred in welding seam, underfills, microcracks and microstructural transformations. Fractures in welded joints occurred in weld zone after the tensile test.
3. It has been concluded that no major differences were observed between tensile strengths of samples joined with different welding parameters and subjected to two different heat treatment procedures. The main reasons for such a result were presence of porosities and heat treatment temperatures were lower than β transus temperature that caused lack of any major change in prior- β grain sizes.
4. Impact toughness was higher in samples joined with lower welding speed or higher laser welding power, in other words higher heat input, (samples B1 and A1) and aged samples (samples A1 and A2). Along with increased heat input via lower welding speed and higher laser power, impact toughness was improved as a result of transformation of martensitic structure to acicular α or Widmanstatten α grain structure.
5. In terms of hardness values of samples joined with different heat inputs, hardness of weld metal and HAZ was higher than the base metal. A hardness increase especially in weld metal occurred as a result of decreased β phase structure due to post-weld heat treatments.

Acknowledgement

Authors thank to Prof. Dr. Zafer TATLI and research assistants of Sakarya University, Faculty of Technology, Metallurgical and Materials Engineering Department, to Prof. Dr. Uğur KÖLEMEN, Assoc. Prof. Dr. Fikret YILMAZ and research assistants of Gaziosmanpaşa University Faculty of Applied Sciences, and KİTAM of Samsun 19 Mayıs University for their valuable contributions.

REFERENCES

[1] M.J. Donachie, Titanium: A Technical Guide, ASM International, Materials Park, Ohio (2000).

[2] F. Karimzadeh, M. Heidarbeigy, A. Saatchi, J. Mater. Process. Technol. **206** (1-3), 388-394 (2008).

[3] N. Kahraman, Mater. Des. **28** (2), 420-427 (2007).

[4] N. Kahraman, B. Gülenç, F. Fındık, J. Mater. Process. Technol. **169** (2), 127-133 (2005).

[5] A. Yıldız, Y. Kaya, N. Kahraman, Int. J. Adv. Manuf. Technol. **86** (5), 1287-1298 (2016).

[6] E. Akman, A. Demir, T. Canel, T. Sınmazçelik, J. Mater. Process. Technol. **209** (8), 3705-3713 (2009).

[7] X. Cao, M. Jahazi, Opt. Lasers. Eng. **47** (11), 1231-1241 (2009).

[8] A.S.H. Kabir, X. Cao, J. Gholipour, P. Wanjara, J. Cuddy, A. Birur, M. Medraj, Metall. and Mat. Trans. A **43** (11), 4171-4184 (2012).

[9] C. Köse, R. Kaçar, Mater. Des. **64**, 221-226 (2014).

[10] C. Köse, R. Kaçar, Mater. Test. **54** (10), 779-785 (2014).

[11] C. Köse, R. Kaçar, J. Fac. Eng. Archit. Gaz. **3** (2), 225-235 (2015).

[12] C. Köse, R. Kaçar, A.P. Zorba, M. Bağırova, A.M. Allahverdiyev, Mater. Sci. Eng. C **60**, 211-218 (2016).

[13] C. Köse, R. Kaçar, Int. J. Electrochem. Sci. **11** (3), 2762-2777 (2016).

[14] C. Köse, Int. J. Electrochem. Sci. **11** (4), 3542-3554 (2016).

[15] C. Köse, Mater. Test. **58** (11-12), 963-969 (2016).

[16] M. Taskin, U. Caligulu, M. Turkmen, Mater. Test. **53** (11-12), 741-747 (2011).

[17] L. Quintino, A. Costa, R. Miranda, D. Yapp, V. Kumar, C.J. Kong, Mater. Des. **28**, 1231-1237 (2007).

[18] K.K. Murthy, S. Sundaresan, J. Mater. Sci. **33** (3), 817-826 (1998).

[19] Y. Liu, S. Tang, G. Liu, Y. Sun, J. Hu, Int. J. Electrochem. Sci. **11** (11), 10561-10580 (2016).

[20] G. Thomas, V. Ramachandra, R. Ganeshan, R. Vasudevan, J. Mater. Sci. **28** (18), 4892-4899 (1993).

[21] S. Sundaresan, G.D.J. Ram, Sci. Technol. Weld. Joi. **4** (3), 151-160 (1999).

[22] T. Mohandas, M. Sirinivas, V.V. Kutumba Rao, Fatigue Fract. Eng. Mater. Struct. **23** (1), 33-38 (2000).

[23] T. Mohandas, D. Banerjee, V.V. Kutumba Rao, Metall. and Mat. Trans. A. **30** (13), 789-798 (1999).

[24] V.A. Kumar, R.K. Gupta, S.K. Manwatkar, P. Ramkumar, P.V. Venkitakrishnan, J. Mater. Eng. Perform. **25** (6), 2147-2156 (2016).

[25] N.K. Babu, S.G.S. Raman, C.V.S. Murthy, G. Madhusudhan Reddy, Mat. Sci. Eng. A **471** (1-2), 113-119 (2007).

[26] C. Köse, E. Karaca, Metals. **7** (6), 221 (2017).

[27] L.W. Tsay, C.Y. Tsay, In. J. Fatigue. **19** (10), 713-720 (1997).

[28] J. Huez, C. Buiriette, E. Andrieu, S. Perusin, S. Audion, Mater. Sci. Forum. **654-656**, 890-893 (2010).

[29] Y. Zhang, Y.S. Sato, H. Kokawa, S.H.C. Park, S. Hirano, Mat. Sci. Eng. A **485** (1-2), 448-455 (2008).

[30] S.H. Wang, M.D. Wei, L.W. Tsay, Mater. Lett. **57** (12), 1815-1823 (2003).

[31] T. Mohandas, D. Banerjee, V.V.K. Rao, Mat. Sci. Eng. A **289** (1), 70-82 (2000).

[32] C. Köse, E. Karaca, Effect of solution and ageing heat treatments on the microhardness and impact toughness properties of fiber laser welded Ti-6Al-4V alloy, 8th International Advanced Technologies Symposium (IATS'17), Turkey (2016).

[33] J.L. Barreda, F. Santamaria, X. Azpiroz X, A.M. Irisarri, J.M. Varona, Vacuum **62** (2-3), 143-150 (2001).